Preprints of the 19th World Congress
The International Federation of Automatic Control
Cape Town, South Africa. August 24-29, 2014

Channel Estimation and Interpolation for Fourth Generation Mobile Broadband Telecommunications

Mauricio G. Cea * **Graham C. Goodwin** ** **Rodrigo Carvajal** ***
Richard H. Middleton **** **Kaushik Mahata** † **Robert S. Karlsson** ‡

* *School of Electrical Engineering and Computer Science, University of Newcastle, 2308, Australia (e-mail: Mauricio.Cea@uon.edu.au).*
** *School of Electrical Engineering and Computer Science (e-mail: Graham.Goodwin@newcastle.edu.au)*
*** *Department of Electronics Engineering, University Santa María, Valparaíso, Chile (e-mail: Rodrigo.Carvajal@usm.cl).*
**** *School of Electrical Engineering and Computer Science, University of Newcastle, 2308, Australia (e-mail: Richard.Middleton@newcastle.edu.au).*
† *School of Electrical Engineering and Computer Science, University of Newcastle, 2308, Australia (e-mail: Kaushik.Mahata@newcastle.edu.au).*
‡ *LTE Research, Ericsson AB, Sweden.(e-mail: Robert.s.Karlsson@ericsson.com).*

Abstract: This paper studies the problem of channel estimation for the downlink in broadband LTE communications. A Kalman Filter is used to combine channel soundings made with pilot tones that are deployed at different times and in different frequency bands on a pre-selected pattern. This Kalman filter is presented in a form directly suitable for implementation as a periodically time varying filter, in the case where periodic pilot tone data is available. Simulation results illustrate the efficacy of this approach.

Keywords: Time-Frequency, Channel Estimation, Kalman Filter, Telecommunications, Linear Estimation, Frequency domain estimation.

1. INTRODUCTION

Fourth generation telecommunications or Long Term Evolution (LTE) represents an evolution of the widespread WCDMA based Universal Mobile Telecommunications System (UMTS) system. LTE uses different modulation and access techniques for the uplink and downlink. Orthogonal Frequency Division Multiple Access (OFDMA) is used in the downlink and Single Carrier Frequency Division Multiple Access (SC-FDMA) is used in the uplink. LTE includes the flexibility to allocate different frequency bands to each user, depending upon the perceived channel quality, and the use of more antennas at the transmitter and the receiver. However, this flexibility is also accompanied by several challenges.

Some problems raised by the extra flexibility of LTE systems include the following: (i) How does the base-station learn which channels are good, and, conversely, which channels are bad for a particular user? (ii) What overhead is involved in testing different channels? (iii) What overhead is involved in the base station allocating resources to users? (iv) Are there inevitable delays in determining and transmitting the relevant channel information and how do these delays impact performance? These are some of the challenges arising in the so called Link Adaptation (LA) problem. All of this depends upon the channel state, for which a suitable model is needed.

In this paper, a periodic Kalman Filter based approach is used to obtain the channel estimate. Several other authors have proposed the use of non-periodic Kalman filters for channel estimation in the literature. Some existing Kalman filtering ideas can be found in (Aronsson, 2011; Dai et al., 2012a,b; Gupta et al., 2012; Sternad et al., 2007). One popular approach for employing Kalman filtering is to model the individual sub-channel gain $H_k(t)$ for a fixed k as an autoregressive process. Unlike these methods we prefer to work with the complete channel response vector $\mathbf{h}(t)$. This allows us to capture the correlations that exist both on a frequency basis and on a sample time to sample time basis. To the best of the authors knowledge this idea has not been previously explored in the literature.

The current paper is the result of a collaboration project with LTE Researh, Ericsson AB and is based on confidential technical reports Goodwin et al. (2012); Mahata and Middleton (2012); Cea et al. (2013); Goodwin et al. (2013).

In the next section, we describe a standard channel model. In section 3, we specialize this channel model to LTE systems. In section 4 we describe an alternative model which is motivated by systems and control theory considerations. Section 5 describes the application of the periodic Kalman filter to the problem of channel estimation. Section 6 presents several simulations examples. Conclusions are presented in section 7.

2. CHANNEL MODELS

A general time-invariant (time-domain) channel model is

$$r(t) = \sum_{\xi=0}^{\Xi} h(\xi)x(t-\xi) + \eta(t), \tag{1}$$

where $r(t)$ is the received signal at sample t, x is the transmitted signal, $\{h(\xi)\}$ is the channel impulse response (CIR), η is the channel noise, and Ξ is the length in samples of the channel impulse response.

The model in (1) needs to be embellished for particular problems. In particular, the model (1) assumes that the CIR is constant for all time. In practice, due to both user mobility, and changing environments, we must allow for time varying channels. A commonly used model to capture channel variations is as follows (see e.g. Jakes (1975); Li et al. (1998)):

$$r(t) = \sum_{\xi=0}^{\Xi} h(t,\xi)x(t-\xi) + \eta(t), \tag{2}$$

where $h(t,\xi)$ is a time-varying impulse response that depends upon two time variables, namely t (the present time) and ξ (the time shift). The underlying assumption here is that variations of h with respect to t are much slower than the time scales ξ of the impulse response.

We can then define the time-dependent Fourier transform:

$$\mathscr{H}(t,\omega_\xi) = \sum_{\xi=0}^{\infty} e^{-j\xi\omega_\xi} h(t,\xi). \tag{3}$$

We assume that $\mathscr{H}(t,\omega_\xi)$ is a random variable. In this context, it is customary to assume that we can write

$$\mathscr{E}\{\mathscr{H}(t,\omega_\xi)\mathscr{H}^*(\bar{t},\bar{\omega}_\xi)\} = \Omega\left(t-\bar{t}\right)\Lambda(\omega_\xi - \bar{\omega}_\xi), \tag{4}$$

where $\mathscr{E}\{\cdot\}$ denotes statistical expectation and $()^*$ denotes complex conjugation.

The two functions $\Omega(\cdot)$ and $\Lambda(\cdot)$ are also traditionally modelled in a particular way (see e.g. Li et al. (1998)). There are several models. One of these is Jakes' model (see Jakes (1975)) where

$$\Omega(\tau) = J_0(\omega_d \tau), \tag{5}$$

where $J_0(\cdot)$ is the zeroth-order Bessel function of the first kind (see e.g Abramowitz and Stegun (1970)) and ω_d is a "constant" (the Doppler angular frequency) given by

$$\omega_d = 2\pi T f_d, \tag{6}$$

where f_d is the Doppler frequency shift and T is the sampling period of the system. Notice that in OFDM systems, T corresponds to the OFDM symbol duration (the inverse of the subcarrier spacing).

We can also define the Fourier Transform of $\Omega(\cdot)$ as

$$\tilde{\Omega}(\omega_t) = \sum_{\tau=-\infty}^{\infty} e^{-j\omega_t\tau}\Omega(\tau) = \begin{cases} \frac{2}{\omega_d}\frac{1}{\sqrt{1-\left(\frac{\omega_t}{\omega_d}\right)^2}} & ; |\omega_t| < \omega_d \\ 0 & ; \text{otherwise} \end{cases} \tag{7}$$

3. SPECIALIZATION TO LTE

We now discuss several important parameters in the previous (general) description of channel models to the *downlink* in LTE. It is convenient to think in terms of "resource blocks". A resource block in LTE is a frequency/time grid that consists of 12 subcarriers and 7 OFDM symbols (i.e. $180\,\text{k[Hz]} * 0.5\,\text{m[s]}$ for a specific case where the subcarrier spacing is $15\,\text{k[Hz]}$ and an OFDM symbol has a duration of approximately 71 m[s], including the cyclic prefix).

We will assume a $20\,\text{M[Hz]}$ bandwidth with 100 consecutive resource blocks in the frequency domain, for which the sampling frequency is $f_s = 30.72\text{M[Hz]}$. Thus, the sampling time is given by

$$T_s = \frac{1}{30.72 \times 10^6}\,\text{[s]} = 32.55\,\text{n[s]}$$

In this case, an OFDM symbol consists of 2048 samples. The length of the cyclic prefix is equal to 144 samples, then the LTE symbol consists of $2048+144 = 2192$ samples. Hence, the LTE symbol time is given by

$$\begin{aligned} t_S &= \frac{2048\text{ samples}}{30.72\,\text{M[Hz]}} + \frac{144\,\text{samples}}{30.72\,\text{M[Hz]}} \\ &= 66.7 + 4.7\,\mu\text{s}. \\ &= 71.4\,\mu\text{s}. \end{aligned}$$

We can now think of the *downlink* LA problem as assigning resource blocks to users. Note that in fact LA also deals with other degrees of freedom, e.g. modulation scheme, number of antennas, error correction code, etc. However, these issues will not be addressed here. The allocation of resource blocks to users depends upon the perceived (or estimated) channel quality.

3.1 Channel estimation

Channel estimation is a critical part of channel quality estimation and is carried out with the aide of transmission of specific pilot tones. There are several sounding strategies that can be used to generate these tones. In LTE, the maximum sounding bandwidth is configured on a cell-wide basis. Eight Cell Reference Signal (CRS) configurations are available, with a specific value for each configuration dependent on the system bandwidth. For example, a user can be assigned the full spectrum or only a fraction of it. The strategy chosen depends upon power saturation, QoS requirements and the number of users in the system.

3.2 A preliminary time/frequency model

The fading spectrum is generally smooth in both the frequency and time domains. Also, the fading spectrum will be different for each user. Hence, we envisage an example of the fading spectrum as shown in Figure 1 (Dahlman et al., 2011, pag. 98):

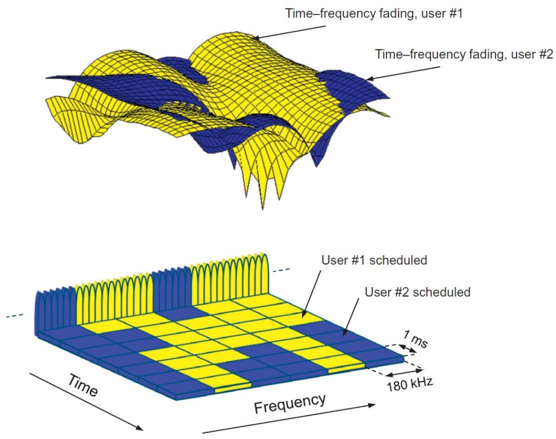

Fig. 1. Example multi-user time frequency fading diagram (Dahlman et al., 2011, pag. 98)

4. A THEORETICAL MODEL FOR FADING

We next describe a theoretic model for fading. Here we depart from the usual models deployed in the telecommunications literature to better align the work with control theory methods.

A related model is described in Özen and Zoltowski (2001) for the case of single carrier systems. The above model extends the idea to multicarrier systems.

4.1 The model

We let $\mathbf{h}(t) \in \mathbb{C}^L$ be the L dimensional vector of complex channel impulse response coefficients $[h_0, h_1, ..., h_{L-1}]$ at time t. We then propose a model for the time variations in the channel of the form

$$\mathbf{h}(t+1) = \mathbf{A}\mathbf{h}(t) + \mathbf{B}\mathbf{w}(t), \tag{8}$$

where $\mathbf{w}(t)$ is a zero mean circular complex white noise sequence, with $\mathscr{E}\{\mathbf{w}(t)\mathbf{w}(t)^H\} = \sigma_w^2\mathbf{I}$; $(.)^H$ denotes the conjugate transpose of a matrix or vector, and $\mathbf{I}$ is the identity matrix. We choose $\mathbf{A}$ as a diagonal matrix where $\lambda_1, \ldots, \lambda_L$ describes the time persistence of the impulse response; and the selection of $\mathbf{B}$ permits various forms of correlation or non-uniform variance to be introduced.

$$\mathbf{A} = \begin{bmatrix} \lambda_1 & 0 & \ldots & 0 \\ 0 & \lambda_2 & \ddots & \vdots \\ \vdots & \ddots & \ddots & 0 \\ 0 & \ldots & 0 & \lambda_L \end{bmatrix}. \tag{9}$$

$$\mathbf{B} = \begin{bmatrix} (1-\lambda_1^2)^{1/2} & 0 & \ldots & 0 \\ 0 & (1-\lambda_2^2)^{1/2} & \ddots & \vdots \\ \vdots & \ddots & \ddots & 0 \\ 0 & \ldots & 0 & (1-\lambda_L^2)^{1/2} \end{bmatrix}. \tag{10}$$

The corresponding channel frequency response is obtained from the Fourier transform. Thus, we have

$$\mathscr{H}(t) = \mathbf{Fh(t)}, \tag{11}$$

where $\mathbf{F}$ is the Discrete Fourier Transform matrix, having (k, l) entry defined by:

$$F(k,l) = \frac{1}{\sqrt{N_C}} e^{-j2\pi \frac{(k-1)(l-1)}{N_C}}, \tag{12}$$

where $k = 1, 2, ..., N_C, l = 1, 2, ..., L$, and N_C is the number of subcarriers. Note that similar approaches have been used in Aronsson (2011) and further study concerning accuracy is discussed.

Notice that the dimension of $\mathscr{H}(t)$ will be typically much larger than the dimension of $\mathbf{h}(t)$ (for example, $N_C = 2048$ versus $L = 10$). This fact allows one to interpolate one part of the frequency response to another part of the frequency response.

We assume that the channel gains (in the frequency domain) are measured using pilot tones)] at N_0 specific frequencies, having index $\hbar_1, ..., \hbar_{N_0}$ at time t. Then, the output (or *measurement*) equation can be written as:

$$\mathbf{y}(t) = \bar{\mathbf{C}}(t)\mathbf{F}\mathbf{h}(t) + \boldsymbol{\eta}'(t) = \mathbf{C}(t)\mathbf{h}(t) + \boldsymbol{\eta}'(t), \tag{13}$$

where $\mathbf{y}(t) \in \mathbb{C}^{N_0}$, $\bar{\mathbf{C}}(t)$ has p, q entries given by

$$\bar{C}_{(p,q)} = \begin{cases} 1, & \text{if } \hbar_p = q \\ 0, & \text{otherwise} \end{cases}. \tag{14}$$

Notice that $\bar{\mathbf{C}}(t)$ is an $N_0 \times L$ matrix.

In equation (13), $\boldsymbol{\eta}'(t)$ denotes a white measurement noise sequence with covariance $\sigma_{\eta'}^2$.

5. PERIODIC KALMAN FILTER

An advantage of the model (13) is that it immediately allows us to use control-theoretic ideas, e.g. periodic Kalman filtering (see Aronsson (2011) for an example), to carry out a number of tasks related to LA, e.g.:

(i) Given the past observations $\{\mathbf{y}(t), \mathbf{y}(t-1), \mathbf{y}(t-2), \ldots\}$, estimate $\mathbf{h}(t)$ and hence $\mathscr{H}(t)$. We denote these estimate as $\hat{\mathbf{h}}(t|t)$ and $\hat{\mathscr{H}}(t|t)$. We note that they can be obtained from a standard (time-varying) Kalman filter.

(ii) We can predict the value of $\mathbf{h}(t)$ and $\mathscr{H}(t)$ at the future time instants, $t + m$, $m > 0$. This prediction is needed for *downlink* channel-dependent resource scheduling. Of course, the prediction error (variance) increases the longer the future prediction horizon m is.

The form of the appropriate prediction equations can be broken in two parts, namely state update (or prediction step)

$$\hat{\mathbf{h}}(t|t-1) = \mathbf{A}\hat{\mathbf{h}}(t-1|t-1) \tag{15}$$

$$\boldsymbol{\Sigma}(t|t-1) = \mathbf{A}\boldsymbol{\Sigma}(t-1|t-1)\mathbf{A}^T + \sigma_w^2\mathbf{I} \tag{16}$$

$$\hat{\mathscr{H}}(t|t-1) = \mathbf{F}\hat{\mathbf{h}}(t|t-1), \tag{17}$$

and measurement update (or filtering step)

$$\tilde{\mathscr{H}}(t) = \mathscr{H}(t) - \bar{\mathbf{C}}(t)\hat{\mathscr{H}}(t|t-1) \quad (18)$$

$$\mathbf{S}(t) = \bar{\mathbf{C}}(t)\mathbf{F}\boldsymbol{\Sigma}(t|t-1)(\bar{\mathbf{C}}(t)\mathbf{F})^T + \sigma_\eta^2 \quad (19)$$

$$\mathbf{K}(t) = \boldsymbol{\Sigma}(t|t-1)(\bar{\mathbf{C}}(t)\mathbf{F})^T\mathbf{S}(t)^{-1} \quad (20)$$

$$\hat{\mathbf{h}}(t|t) = \hat{\mathbf{h}}(t|t-1) + \mathbf{K}(t)\tilde{\mathscr{H}}(t) \quad (21)$$

$$\boldsymbol{\Sigma}(t|t) = (\mathbf{I} - \mathbf{K}(t)\bar{\mathbf{C}}(t)\mathbf{F})\boldsymbol{\Sigma}(t|t-1) \quad (22)$$

$$\hat{\mathscr{H}}(t|t) = \mathbf{F}\hat{\mathbf{h}}(t|t), \quad (23)$$

(iii) We can evaluate the covariance of the estimation errors. Again, this is provided by the Kalman filter (see (22) above). The covariance depends upon the pilot tone allocation sequence $\{\bar{\mathbf{C}}(t)\}$.

(iv) We can design the sequence $\{\bar{\mathbf{C}}(t)\}$ (subject to constraints) to minimize the estimation error. In particular, we note that the covariance of the channel estimation errors satisfy (22). It is clear that $\boldsymbol{\Sigma}(t|t)$ depends upon the sequence $\{\mathbf{C}(t)\}$. Hence, one can ask, " What sequence $\{\mathbf{C}(t)\}$ minimizes an appropriate scalar function of $\boldsymbol{\Sigma}(t|t)$ subject to constraints on $\bar{\mathbf{C}}(t)$? "

Remark 1. In practice, the sounding pattern is typically periodic. In this case, there is no need to solve (16), (19), (20), or (22) on-line. Instead, because of the periodic measurement pattern, the Kalman gains, $K(t)$ will converge to a periodic pattern which can be precomputed (off-line) and then recalled when needed (see Goodwin and Sin (1984)). This precomputation in the periodic case may significantly reduce the computational load for implementing the estimation algorithm, since the most expensive matrix-matrix multiplication steps are removed.

Remark 2. We have implicitly assumed that the User Equipment (UE, e.g. mobile handset) periodically receives and measures the pilot tone data (CRSs). The pilot tones sent by the base station, may have a periodic pattern. In practice, however, the UE will not always 'listen' for these tones, since switching on the UE low noise amplifiers, and performing the required computations creates a significant power drain. In this case, the problem can no longer be treated as periodic (see Remark 1). This situation can be accommodated by omitting the measurement update, steps (18)-(23), when no pilot tone data is available. We would of course expect some deterioration in performance given the reduced information available.

6. EXAMPLES

We illustrate the performance of this approach using two rates of change (slow and moderate) in the channel impulse response. We consider 2048 subcarriers and 10 time taps in the channel impulse response. The configuration used for the pilot tones $\bar{\mathbf{C}}(t)$ corresponds to alternatively sounding the lower and higher frequencies. The channel is not sounded every sampling instant but once every 35 samples. The first 10 taps of the channel impulse response are considered to be zero due to the transmission delay, followed by 10 non zero taps, giving a total of $L = 20$ for the channel impulse response.

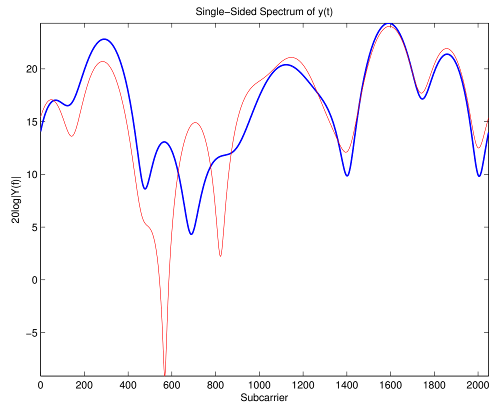

Fig. 2. Channel frequency response immediately after sounding at high frequencies.

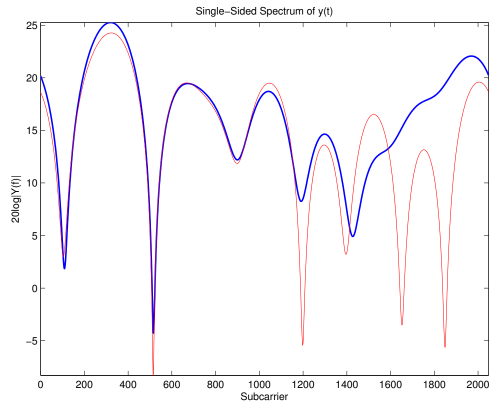

Fig. 3. Channel frequency response immediately after sounding at low frequencies.

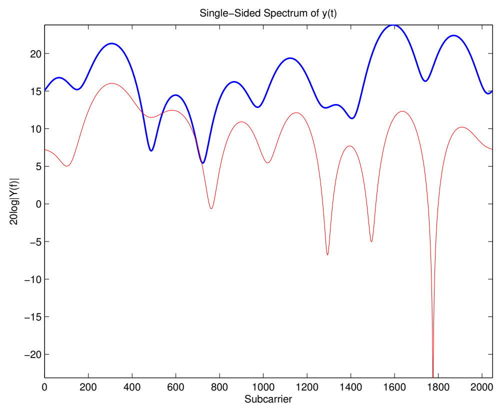

Fig. 4. Channel frequency response just prior to new sounding at high frequencies.

6.1 Moderately Rapidly Fading Channel $\lambda_1, \ldots, \lambda_{20} = 0.97$

Many tests where performed. Here, we show particular results at a specific instant of time.

Figures 2 and 3 show the channel estimates immediately after a measurement is received. The channel

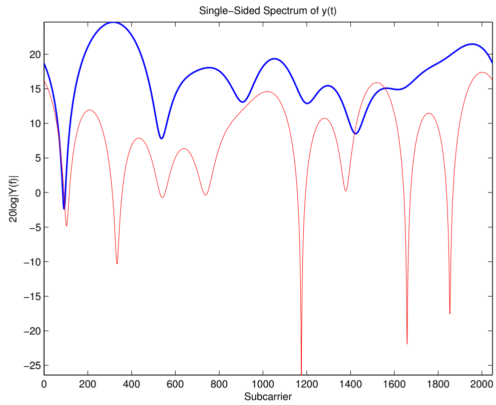

Fig. 5. Channel frequency response just prior to new sounding at low frequencies.

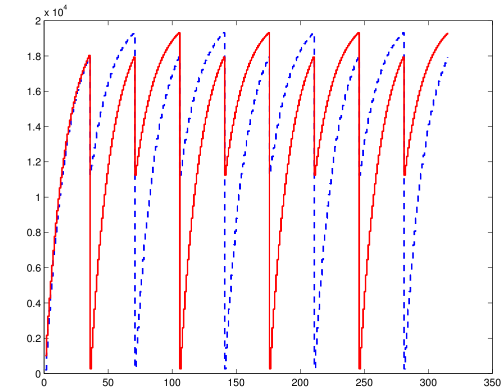

Fig. 6. Total estimate variance of frequency response estimate. Solid Red: Low frequencies. Dashed Blue: High frequencies.

estimates improve for all frequencies but particularly in the region where the sounding signals are applied. In this and subsequent plots the solid blue line is the true frequency response and the solid red line the estimate.

Figures 4 and 5 show the channel estimate just before receiving new data. It can be seen that the estimates have deteriorated significantly because the channel is changing rapidly.

Figure 6 shows the total estimation variance for both set of frequencies at each sampling time. Here it is clearly seen that the estimation variance increase between samples. Furthermore, when a measurement is taken the variance decreases more significantly for the set of frequencies that is sounded. However, the other set of frequencies also decreases its variance. This is due to the correlation, in the frequency domain, of the time-varying channel, that is, one can extract information about other frequencies by using the Kalman filter. The periodic nature of the filter is evident in the figure.

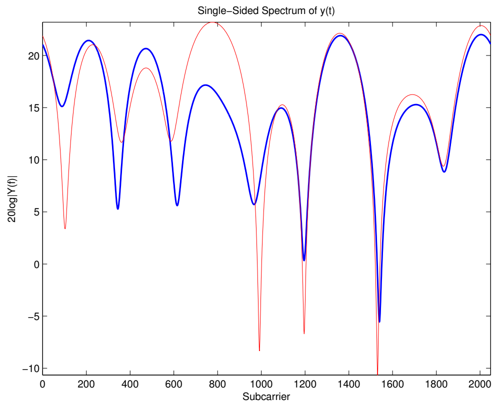

Fig. 7. Channel frequency response immediately after sounding at high frequencies.

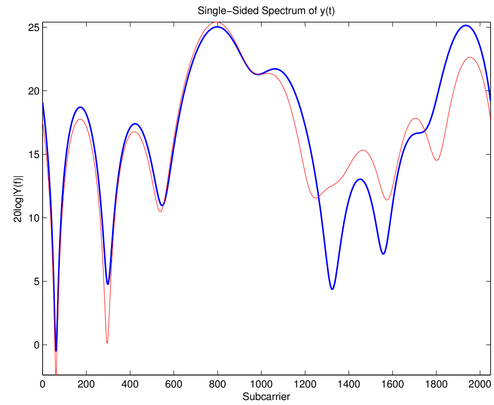

Fig. 8. Channel frequency response immediately after sounding at low frequencies.

6.2 Slowly Changing Channel $\lambda_1, \ldots, \lambda_{20} = 0.99$

Figures 7 and 8 show the estimates when a slowly varying channel is considered. After, waiting for 35 samples to take a new measurement the estimates provide more accurate information than before. Figures 9 and 10 confirm that this approach allows one to successfully predict the channel response at all frequencies.

Figure 11 shows the variances for both set of frequencies. It can be seen that every time a sample is taken the Kalman filter allows one to extract information about the whole spectrum, not only the sounded set. Also, since the channel changes slowly the total estimation variance is also reduced by approximately one order of magnitude.

7. CONCLUSIONS

This paper has studied the use of periodic Kalman Filtering to obtain down link channel estimates from periodically deployed soundings in time and frequency. The methods are aimed at aspects of link adaptation in LTE broadband communications. Simulations have verified the validity of the approach.

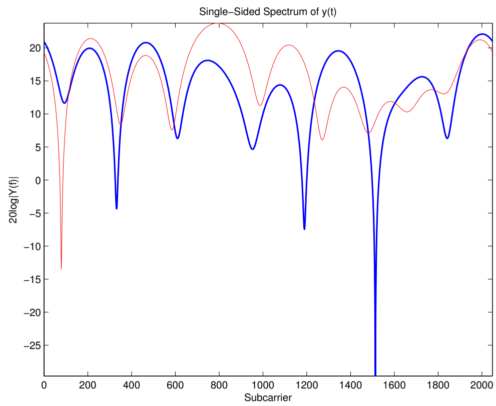

Fig. 9. Channel frequency response just prior to new sounding at high frequencies.

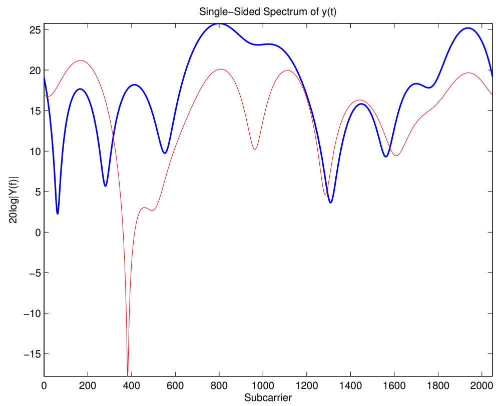

Fig. 10. Channel frequency response just prior to new sounding at low frequencies.

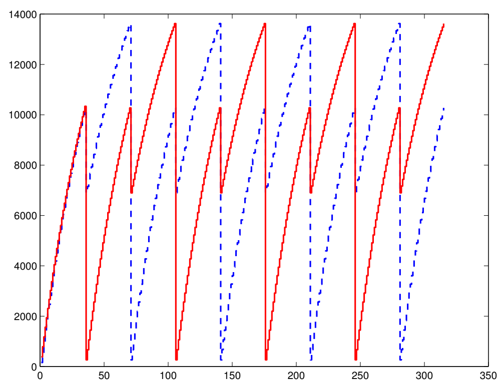

Fig. 11. Total estimate variance of frequency response estimate. Solid Red: Low frequencies. Dashed Blue: High frequencies.

ACKNOWLEDGEMENTS

The authors would like to acknowledge financial support from LTE Research, Ericsson AB in Sweden and the Australian Research Council Linkage Project LP1202000321.

REFERENCES

Abramowitz, M. and Stegun, I. (1970). Handbook of mathematical functions.

Aronsson, D. (2011). Channel estimation and prediction for mimo ofdm systems: Key design and performance aspects of kalman-based algorithms.

Cea, M., Goodwin, G., and Middleton, R. (2013). Uplink channel estimation. *Confidential Report*.

Dahlman, E., Parkvall, S., and Skold, J. (2011). *4G: LTE/LTE-Advanced for Mobile Broadband: LTE/LTE-Advanced for Mobile Broadband*. Academic Press.

Dai, L., Wang, Z., Wang, J., and Yang, Z. (2012a). Joint time-frequency channel estimation for time domain synchronous ofdm systems. *IEEE Transactions on Broadcasting*.

Dai, X., Zhang, W., Xu, J., Mitchell, J.E., and Yang, Y. (2012b). Kalman interpolation filter for channel estimation of lte downlink in high-mobility environments. *EURASIP Journal on Wireless Communications and Networking*, 2012(1), 1–14.

Goodwin, G., Carvajal, R., and Agüero, J. (2012). An LTE downlink channel model for link adaptation. *Confidential Report*.

Goodwin, G., Cea, M., and Middleton, R. (2013). Further notes on LTE channel estimation for uplink and downlink. *Confidential Report*.

Goodwin, G.C. and Sin, K. (1984). *Adaptive Filtering Prediction and Control*. Prentice Hall, Englewood Cliffs, New Jersey.

Gupta, A., Pathela, M., and Kumar, A. (2012). Kalman filtering based channel estimation for mimo-ofdm. *International Journal of Computer Applications*, 53(15), 8–12.

Jakes, W.C. (1975). Microwave mobile communications.

Li, Y., Cimini Jr, L.J., and Sollenberger, N.R. (1998). Robust channel estimation for ofdm systems with rapid dispersive fading channels. *Communications, IEEE Transactions on*, 46(7), 902–915.

Mahata, K. and Middleton, R. (2012). LTE channel estimation. *Confidential Report*.

Özen, S. and Zoltowski, M.D. (2001). A fading filter approximation to enable state-space modeling and joint data channel estimation of (time-varying) frequency selective channels with antenna arrays. In *IEEE Circuits and Systems Society Notre Dame Workshop on Wireless Communication and Networking, South Bend, IN*.

Sternad, M., Svensson, T., Ottosson, T., Ahlén, A., Svensson, A., and Brunstrom, A. (2007). Towards systems beyond 3g based on adaptive ofdma transmission. *Proceedings of the IEEE*, 95(12), 2432–2455.